ELSEVIER

Journal of Nuclear Materials 248 (1997) 220–225

journal of nuclear materials

Radiation effect on the chemical state of fission product iodine

Kenji Konashi [a,*], Yoshinobu Siokawa [a], Hideo Kayano [a], Michio Yamawaki [b]

[a] *The Oarai Branch, Institute for Materials Research, Tohoku University, Oarai, Ibaraki 311-13, Japan*

[b] *Nuclear Engineering Research Laboratory, Faculty of Engineering, University of Tokyo, Hongo, Bunkyo-ku, Tokyo 113, Japan*

Abstract

The chemical states of fission products in nuclear fuel pins are usually evaluated by thermodynamic analysis. The thermal equilibrium is assumed in the analysis, so that atoms included in the system are to obey Maxwell–Boltzmann energy distribution. However, nuclear fuel pins are subjected to a strong radiation field and, hence, molecules in the system have non-equilibrium energy distribution, which may affect the chemical state of fission products. In this paper, collision processes initiated by fission fragments in a solid fuel were calculated by the TRIM Monte Carlo code. In the gas phase in a fuel-cladding gap, the same processes were also simulated. Based on the calculation results, it has been evaluated how the energy distribution of gas atoms in fuel-cladding gap is different from Maxwell–Boltzmann distribution corresponding to the temperature of the system. It has been concluded that the radiation effect of fission fragments on chemical reactions are significant when the threshold energy of the chemical reaction is high and the reaction occurs at low temperature. The radiation effect on the decomposition reaction of CsI vapor has been demonstrated at 650 K, a fission density of 4×10^{13} fissions cm^{-3} s^{-1} and a Xe pressure of 10 atm in the fuel-cladding gap. The CsI decomposition reaction rate has been found to increase the iodine partial pressure from 3.7×10^{-23} atom in the absence of radiation to 3.1×10^{-10} atoms in the radiation field. © 1997 Elsevier Science B.V.

1. Introduction

The chemical state of fission products in nuclear fuel pins is usually evaluated by thermodynamic analysis, where the thermal equilibrium is assumed and atoms included in a reaction system obey the Maxwell–Boltzmann energy distribution. However, nuclear fuel pins are subjected to a strong radiation field, where a large number of energetic atoms are produced. The energy distribution of atoms in nuclear fuel pins is different from that in the thermal equilibrium system.

Being high-energy charged particles, fission fragments are considered as a radiation source in this work. Fission fragments produce energetic recoil atoms on elastic collisions with stationary atoms of the fuel crystal lattice. The recoil atoms can also transfer kinetic energies to other atoms of the lattice as well as to gas atoms in the fuel-cladding gap by elastic collisions, creating secondary and in turn, higher-order energetic atoms, that is, the collision cascade. An effect of the energetic atoms on a chemical reaction in the nuclear fuel pin has been studied.

Gas phase chemical reaction in fuel-cladding gap is important not only for a study of cladding inner corrosion in normal operation [1–3] but also for an evaluation of the source term of radioactive fission products under accident conditions [4]. A chemical reaction rate in the radiation field can be calculated based on the gas kinetic theory in case of a flux of energetic atoms. General formulae of the gas reaction theory are summarized in Section 2. Fluxes of energetic atoms in the fuel-cladding gap are estimated.

In previous papers [5,6], preliminary estimations of fluxes of energetic atoms induced by fission fragment were made. Fluxes were calculated by deterministic methods using isotropic cross-section of energy transfer collision for the simplified geometry of the fuel-cladding gap. The deterministic method allows treatment of only one element for the transport medium. In this study, the same problem

* Corresponding author. Tel.: +81-29 267 3181; fax: +81-29 267 4947; e-mail: konashi@ob.imr.tohoku.ac.jp.

PII S0022-3115(97)00121-9

is again solved by using a Monte Carlo simulation code, with which collision processes initiated by fission fragments can be simulated theoretically. The Monte Carlo code is particularly useful for solving complex problems that cannot be modeled by the deterministic methods. The flux of each component of fuel, U or O, is estimated. The flux is also calculated as a function of the distance from the fuel surface. The procedure of Monte Carlo calculation is described in Section 3. It is shown in Section 4 how different the energy distribution of the radiation induced flux of energetic atoms in nuclear fuel pins is from that of gas atoms in the thermal equilibrium system.

As an example, the decomposition reaction rate of CsI vapor in the radiation field was estimated using the calculated flux of energetic atoms induced by the fission fragments. The CsI vapor is an important compound in evaluating chemical state of iodine in fuel pins. According to thermodynamic estimation, fission product iodine tends to react with fission product cesium of which fission yield is about ten times greater than that of iodine, resulting in the formation of a thermodynamically stable compound, cesium iodide. The increase of iodine partial pressure by decomposition of CsI vapor in the radiation field is discussed in Section 5.

2. Reaction rate in gas phase

A gas phase reaction rate, k ($cm^3\ s^{-1}$), between atom A and B can be calculated by using relative velocity, cross-section and the velocity distribution of each particle,

$$k = \int\int v_r \sigma(v_r) f_A(v_A) f_B(v_B)\, d\vec{v}_A\, d\vec{v}_B, \qquad (1)$$

where v_r is the relative velocity ($cm\ s^{-1}$), v_A and v_B are the velocities of atoms A and B, respectively ($cm\ s^{-1}$), $\sigma(v_r)$ is the reaction cross-section (cm^2), $f_A(v_A)$ and $f_B(v_B)$ are the velocity distributions of A and B, respectively.

The velocity distribution can be calculated by

$$f_{A\,or\,B}(v_{A\,or\,B}) = \Phi_{A\,or\,B}(E)/\rho_{A\,or\,B} v_{A\,or\,B}, \qquad (2)$$

where $\Phi_{A\ or\ B}(E)$ is the particle flux, $\rho_{A\ or\ B}$ is the density of the particle and $v_{A\ or\ B}$ has the same meaning as in Eq. (1).

In the case of thermal equilibrium conditions, the reaction rate is calculated by assuming the Maxwell–Boltzmann distribution. The velocity distribution in the gap of a nuclear fuel pin, where strong radiation field produces energetic gas atoms, is different from the Maxwell–Boltzmann distribution. In the present paper, the radiation induced flux of energetic particles is calculated by the Monte Calro simulation code and the velocity distribution is calculated by Eq. (2). The reaction rate in the radiation field is obtained by numerical integration of Eq. (1).

3. Monte Carlo simulation of collision cascade

The collision processes in nuclear fuel pins have been simulated with the Monte Carlo code, TRIM [7], with which the two-dimensional ion penetration in non-structured materials can be calculated. Fig. 1 schematically shows the evolution of collision cascades in UO_2 fuel and in the fuel-cladding gap. Fission fragments in the form of high-energy charged particles were considered as a radiation source. Fission fragments produce the collision cascades in the fuel, where some recoiled atoms are emitted the fuel-cladding gap. When the emitted atom has a large energy, another collision cascade of Xe atoms is also generated in the fuel-cladding gap.

At a fission event, the fission fragment is born in the fuel with a high energy of ~ 80 MeV. On the other hand, chemical reactions mainly occur on collision with particles of low energy of some eV. A number of collision events at low energy are included in the collision cascade generated by the fission fragment. It takes a large computation time to simulate collision processes ranging in energy from MeV to eV. To reduce the computation time, the numerical calculations are carried out in two steps as shown in Fig. 1, i.e., the simulation of the collision processes in the fuel and those in the fuel-cladding gap.

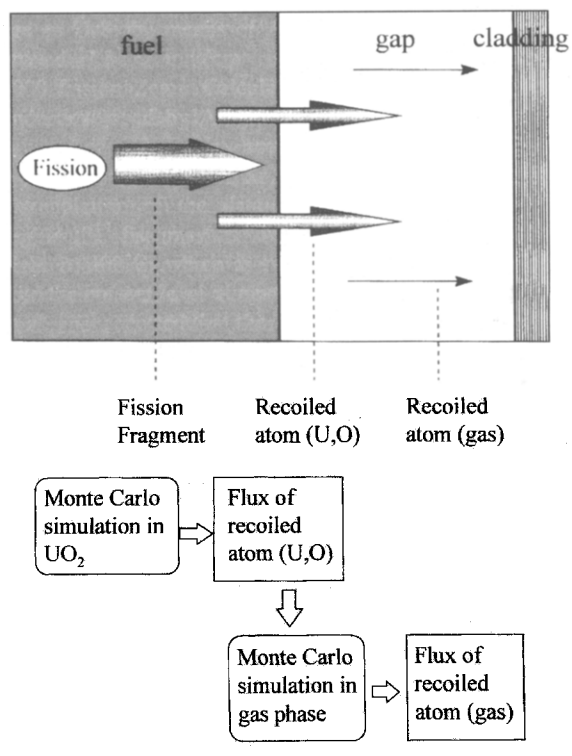

Fig. 1. Evolution of recoil atom fluxes.

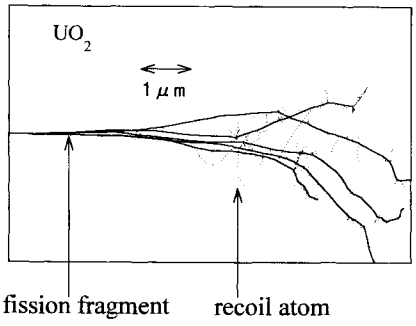

Fig. 2. Trajectories of fission fragments and recoil atoms in UO_2 (TRIM code).

3.1. Collision cascade in UO_2 fuel

Fig. 2 shows an example of a TRIM calculation of a collision cascade in UO_2. Solid lines show trajectories of fission fragments, while dotted lines are those of recoil U and O atoms. In the Monte Carlo simulation, a particle moves over some distance (track length) with a constant energy between collision events. The particle flux generated by fission fragments is calculated by track lengths as follows; the definition of particle flux is

$$\Phi(E) = \rho(E)v, \tag{3}$$

where $\rho(E)$ is the particle density and v is the particle velocity. The particle flux integrated in the volume of the transport media of UO_2 fuel corresponds to summation of the track length generated by fission fragment in unit time. Therefore the volume average fluxes of the particle with the energy of E_M are calculated with

$$\Phi_M(E_M) = 2\dot{F}V\sum_i l_i(E_M)/V = 2\dot{F}\sum_i l_i(E_M), \tag{4}$$

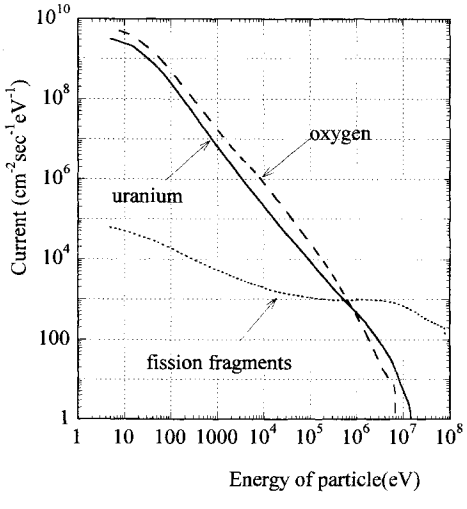

Fig. 3. Currents of atoms emitted from fuel surface for fission density of 4×10^{13} fission s^{-1}.

where M = fission fragment, U or O, while $\Sigma_i l_i(E_M)$ represents the summation of track lengths of particle M with an energy of E_M, $\dot{F}$ is the fission density and V is the volume of transport media (i.e., UO_2 fuel). Currents emitted from the fuel surface, $J_M(E_M)$, are calculated by

$$J_M(E_M) = \Phi_M(E_M)/2. \tag{5}$$

Fig. 3 shows the energy spectra of the currents of oxygen, uranium and fission fragments emitted from the surface of the fuel. In this calculation, $\dot{F}$ was set to be 4×10^{13} fissions cm^{-3} s^{-1}, which corresponds to the fission density in a typical LWR fuel rod operating with a linear heat rate of 300 W/cm. The current of fission fragments is much lower than those of U and O in the low energy region, where the radiation effect on chemical reaction becomes important. The oxygen current is twice as large as the uranium current, because of the atomic composition ratio of UO_2.

3.2. Collision cascade in fuel-cladding gap

In the second step, the collision processes in the gas phase of the fuel-cladding gap were simulated by using the TRIM Monte Carlo code. It was assumed that the fuel-cladding gap with 10 μm in width is filled with fission gas Xe at a pressure of 10 atm. Fig. 4 shows an example of collision cascades in the fuel-cladding gap, which are produced by oxygen and uranium particles emitted from the fuel surface.

In this calculation, the fuel-cladding gap is divided into ten layers with the same thickness of 1 μm each. The flux of energetic Xe atoms is calculated for each layer. The Xe-flux in the layer j (j = 1 to 10), which is generated by recoiled U, is calculated with

$$\Phi_{Xe(U)}(E_{Xe}, j) = \int\Phi_U(E_U)\, S \sum_i l_i(E_U, E_{Xe}, j) \times dE_U/V, \tag{6}$$

where S and V are the area and the volume of each layer.

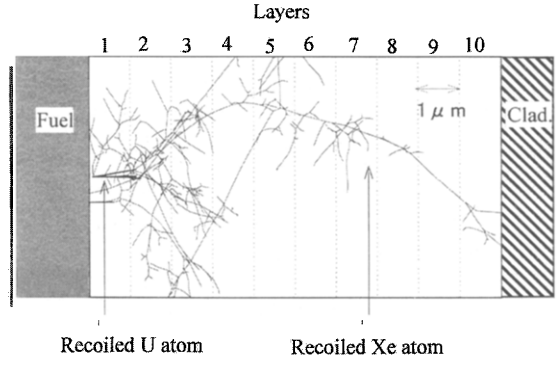

Fig. 4. Trajectories of U-atoms emitted from fuel surface and recoil Xe atoms in fuel-cladding gap.

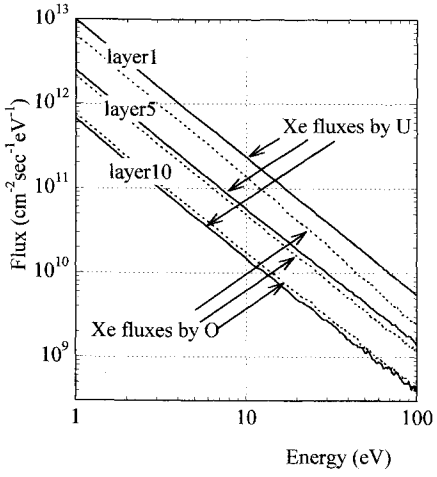

Fig. 5. Flux of energetic Xe-atom generated by recoil U and O atoms.

S/V is calculated to be 10^{-6} cm^{-1}. $\Sigma_i l_i(E_U, E_{Xe}, j)$ is the sum of the track lengths of recoiled Xe with energy of E_{Xe}. E_U is the energy of the U-atom at emission from the fuel surface. Similarly, the Xe-flux generated by recoiled O is calculated with

$$\Phi_{Xe(O)}(E_{Xe}, j) = \int \Phi_O(E_O)\, S \sum_i l_i(E_O, E_{Xe}, j) \times dE_O/V, \quad (7)$$

S, V and $\Sigma_i l_i(E_O, E_{Xe}, j)$ have the same meanings as those in Eq. (6). The total radiation induced flux of Xe atoms in the layer j is obtained by

$$\Phi_{Xe}(E_{Xe}, j) = \Phi_{Xe(U)}(E_{Xe}, j) + \Phi_{Xe(O)}(E_{Xe}, j). \quad (8)$$

Fig. 5 shows the Xe-flux spectra for different layers. The chemical reaction rate is dominated by collision processes at energies close to a low energy reaction threshold. This is the reason why the energy region from 1 to 100 eV was selected in Fig. 5. In layer 1, the Xe-flux generated by U-atoms is larger than that by O-atoms, although the flux of O atoms emitted from fuel surface is larger than the flux of U atoms. The reason is that the cross-section of energy transfer between U and Xe is much larger than that between O and Xe. On the contrary, in layer 10, the Xe-flux by O-atoms is larger than that by U-atoms, since low energy U-atom has a shorter range compared with that of O-atom.

4. Comparison of radiation induced flux with flux in thermal equilibrium

The radiation induced Xe-flux is compared with the thermal Xe-flux without exposure to radiation in Fig. 6. Solid line shows the total radiation induced Xe-flux in the layer 1, which includes both the Xe-flux generated by U-atoms and that by O-atoms. Least-squares fitting of the radiation induced Xe-flux yield a slope of -1.66 for the lines on the log–log plots of flux versus energy such as shown below:

$$\Phi_{Xe}(E_{Xe}) = 0.425 \dot{F} E_{Xe}^{-1.66}. \quad (9)$$

The thermal Xe-flux based on the Maxwell–Boltzmann distribution is expressed with

$$\Phi_{Xe}^{th}(E_{Xe}) = \rho_{Xe}\left(\frac{2}{kT}\right)\left(\frac{E_{Xe}}{kT}\right)^{1/2} \exp\left(\frac{-E_{Xe}}{kT}\right), \quad (10)$$

where k is the Boltzmann constant, T is the temperature of the gas phase and ρ_{xe} has the same meaning as in Eq. (2). As shown in Fig. 6, the thermal Xe-flux (broken line) at 650 K rapidly decreases with increase of particle energy.

Reaction kinetics in the gas phase are dominated by collision processes. For example, collisional decomposition of the molecule occurs when the molecule is excited above its threshold energy of decomposition. It is important to evaluate particle fluxes in gas phase at energies close to the threshold energy. The ratio of the radiation induced Xe-flux to the thermal Xe-flux is shown in Fig. 7 as a function of particle energy for different temperatures. The ratio rapidly increases with increase of particle energy as well as with decrease of temperature. This means that chemical reactions are strongly enhanced by radiation in the following case; the threshold energy of reaction is high and the reaction occurs at relatively low temperatures.

When the thermal flux is equal to the radiation induced flux, i.e., the above ratio is equal to 1 (see the dashed line in Fig. 7), both the fluxes are equivalent to each other as far as the chemical reaction at the particular energy is concerned. For example, the chemical reaction at 2 eV in radiation field is equivalent to the reaction in non-radiation field at temperature of 650 K. The radiation effect on the chemical reaction at energies less than 2 eV is considerably small at about 700 K. Using Fig. 7, it can be judged

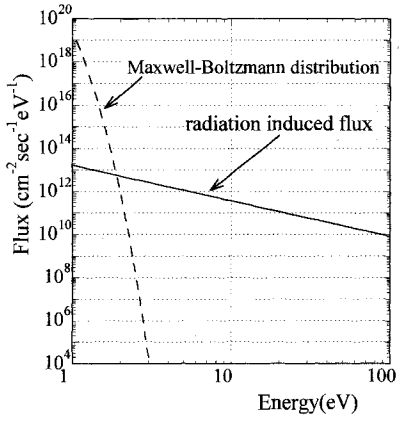

Fig. 6. Comparison between flux in thermal equilibrium and flux in radiation field.

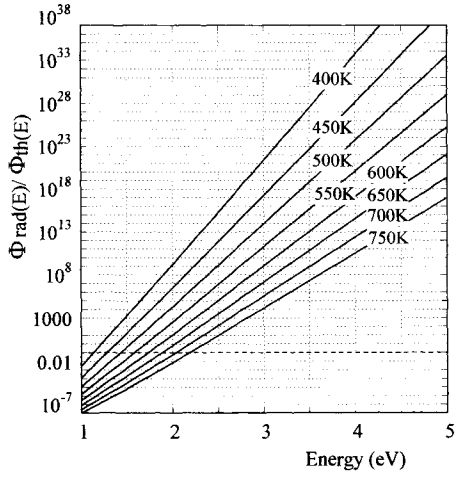

Fig. 7. Ratio of flux in radiation field to flux in thermal equilibrium system as a function of energy for different gas temperatures.

from temperature and reaction energy conditions whether the radiation effect on chemical reaction is significant or not.

5. Application to CsI vapor decomposition reaction

The flux calculated above has been applied to evaluate the CsI vapor decomposition reaction in the radiation field. In the case of CsI vapor, the threshold energy of decomposition is 4.35 eV in a laboratory system [8]. The cross-section of CsI vapor decomposition is expressed with

$$\sigma(E) = C_1(1 - E_{th}/E)e^{C_2T} \quad \text{for } E < 10, \tag{11}$$

$$\sigma(E) = C_1(1 - E_{th}/E)e^{C_2T}\sqrt{C_3/E} \quad \text{for } E \geq 10, \tag{12}$$

where $\sigma(E)$ = cross-section in cm^2, E = energy in eV, $E_{th} = 4.35$ eV, $C_1 = 2.9 \times 10^{-16}$, $C_2 = 2.6 \times 10^{-3}$ and $C_3 = 10$ of T is set to be 650 K.

The decomposition reaction rates have been calculated in two different conditions:

(i) Under the thermal equilibrium condition without radiation, the CsI molecule decomposes due to collision with Xe gas atom as

$$CsI + Xe \rightarrow Cs + I + Xe. \tag{13}$$

Substituting the cross-section of Eqs. (11) and (12) and the thermal Xe-flux of Eq. (10) into Eq. (1), the reaction rate in the non-radiation field, $kd_2[Xe]$, is obtained as 2.8×10^{-13} s^{-1}.

(ii) In the radiation field in nuclear fuel pins, the reaction system contains some energetic particle (Xe^*) generated by radiation of fission fragments. These particles have a potential to decompose CsI molecule such as

$$CsI + Xe^* \rightarrow Cs + I + Xe^*. \tag{14}$$

The reaction rate in the radiation field has been calculated with Eq. (1) using the flux of the energetic particle of Eq. (9). As a result, the reaction rate, $kd_4[Xe^*]$, was obtained as 5.5×10^{-3} s^{-1}.

The partial pressures of iodine in the Cs–I reaction system have been calculated for two different reaction cases of CsI vapor decomposition described above. The calculation has been performed in the same way as in the previous paper [6]; In the fuel-cladding gap, the pressure of Cs can calculated for the equilibrium between UO_2 and Cs_2UO_4 on the surface of fuel. The pressure of CsI vapor is determined as the vapor pressure of solid CsI on the inner surface of cladding. The iodine partial pressure was determined for the following reaction system:

$$Cs + I_2 \underset{kd_1}{\overset{kr_1}{\rightleftarrows}} CsI + I, \tag{15}$$

$$Cs + I + Xe \underset{kd_2}{\overset{kr_2}{\rightleftarrows}} CsI + Xe, \tag{16}$$

$$I + I + Xe \underset{kd_3}{\overset{kr_3}{\rightleftarrows}} I_2 + Xe, \tag{17}$$

$$Cs + I + Xe^* \underset{kd_4}{\leftarrow} CsI + Xe^* + Xe, \tag{18}$$

where Xe plays the role of a third body, which leads to excitation and relaxation of the molecules. The kr_1 to kr_3 and kd_1 to kd_4 are the reaction rate constants. The values of the kr_1 to kr_3 and kd_1 to kd_3 can be determined from the reported experimental results. The iodine partial pressures were obtained by solving simultaneously the rate equations for the above reaction system [6]. To simplify the problem, chemical reactions on the cladding surface and sputtering from the cladding surface were not considered in the present analysis. The other calculation conditions and calculated iodine partial pressures are summarized in Table 1. The calculation results show a large effect of the radiation field on iodine partial pressure.

Table 1
Calculation conditions and results

Calculation conditions	
Temperature of fuel surface	750 K
Temperature of gas phase	650 K
Temperature of cladding inner surface	550 K
Oxygen potential	−400 kJ/mol
Fission density	4×10^{13} fission cm^{-3} s^{-1}
Results	
Partial pressure of iodine (atom)	3.7×10^{-23} atoms in non-radiation field 3.1×10^{-10} atoms in radiation field

6. Conclusion

Sequential collision processes in nuclear fuel pins induced by the radiation of fission fragments have been simulated by a Monte Carlo code. The following conclusions have been obtained from the calculation results.

(1) The radiation induced flux of Xe atoms in a typical fuel-cladding gap is mainly generated by U- and O-atoms emitted from the fuel surface. In the layer of the gas phase close to the fuel surface (within 1 μm distance from the fuel surface), the Xe-flux generated by U-atoms is larger than that by O-atoms. On the contrary, the Xe-flux by O-atoms is larger than that by U-atoms in the gas layer 10 μm apart from the fuel surface.

(2) The radiation induced flux of Xe-atoms in the gas phase within 1 μm distance from the fuel surface has been calculated to be equal to

$$\Phi_{Xe}(E_{Xe}) = 0.425\dot{F}E_{Xe}^{-1.66}\ (\mathrm{cm\ s^{-2}\ eV^{-1}}),$$

where E_{Xe} is energy of Xe atoms in eV and $\dot{F}$ is fission density in fission $\mathrm{cm^{-3}\ s^{-1}}$.

(3) The ratio of the radiation induced flux of Xe-atoms to the thermal equilibrium flux rapidly increases with an increase in the energy of the Xe-atom. The ratio also increases with a decrease in temperature. From these analyses, it can be concluded that chemical reactions are strongly enhanced by radiation in the following case; the threshold energy of chemical reactions is high and the reaction occurs at relatively low temperatures.

(4) Estimation of the radiation effect on the decomposition reaction of CsI vapor has been demonstrated in the case of 650 K, the fission density of 4×10^{13} fissions $\mathrm{cm^{-3}\ s^{-1}}$ and the Xe pressure of 10 atm. Large enhancement due to the radiation field on the decomposition rate of CsI vapor has been confirmed. The radiolysis of CsI vapor increases iodine partial pressure from 3.7×10^{-23} atm in a non-radiation field to 3.1×10^{-10} atm in the radiation field.

References

[1] K. Uematsu, Y. Ishida, K. Koizumi, J. Komatsu, in: Proc. Int. Working Group on Fast Reactors, IWGFR-16 (International Atomic Energy Agency, Tokyo, 1977) p. 79.
[2] M. Aubert, D. Calais, R. Le Beuze, J. Nucl. Mater. 58 (1975) 257.
[3] B. Cox, J.C. Wood, in: Corrosion Problems in Energy Conversion and Generation, ed. C.S. Tedmon, Proc. Electrochemical Soc., 1974, p. 275.
[4] J. Paquette et al., J. Nucl. Mater. 130 (1985) 129.
[5] K. Konashi, M. Yamawaki, T. Yoneoka, J. Nucl. Mater. 160 (1988) 75.
[6] K. Konashi, M. Yamawaki, J. Nucl. Sci. Technol. 29 (1) (1992) 1.
[7] J.F. Ziegler, J.P. Biersack, U. Littmark, The Stopping and Range of Ions in Solid (Pergamon, Oxford, 1985).
[8] F.P. Tully, Y.T. Lee, R.S. Berry, Chem. Phys. Lett. 9 (1971) 80.